

Journal of Visualized Experiments

Assessing TMEM Doorway-Mediated Vascular Permeability Associated with Cancer Cell Dissemination, using Intravital Imaging and Fixed Tissue Analysis --Manuscript Draft--

Article Type:	Invited Methods Article - JoVE Produced Video
Manuscript Number:	JoVE59633R2
Full Title:	Assessing TMEM Doorway-Mediated Vascular Permeability Associated with Cancer Cell Dissemination, using Intravital Imaging and Fixed Tissue Analysis
Keywords:	Intravital Imaging; immunofluorescence; Blood Vessel Permeability; Tumor Microenvironment of Metastasis (TMEM); High Molecular Weight Dextran; Breast cancer; metastasis
Corresponding Author:	Maja Oktay UNITED STATES
Corresponding Author's Institution:	
Corresponding Author E-Mail:	maja.oktay@einstein.yu.edu
Order of Authors:	George S Karagiannis Jessica M Pastoriza Lucia Borriello Rojin Jafari Anouchka Coste John S Condeelis Maja Oktay David Entenberg
Additional Information:	
Question	Response
Please indicate whether this article will be Standard Access or Open Access.	Standard Access (US\$2,400)
Please indicate the city, state/province, and country where this article will be filmed. Please do not use abbreviations.	Bronx, NY, USA



Montefiore

Jack & Pearl Resnick Campus
Price Center 202
1301 Morris Park Avenue
Bronx NY 10461-1975 USA

Department of Anatomy and Structural Biology Gruss Lipper Biophotonics Center

David Entenberg, Ph.D.

*Faculty - Senior Associate
Department of Anatomy & Structural Biology
Director of Technological Development
Director of Integrated Imaging
Integrated Imaging Program
Gruss-Lipper Biophotonics Center*

David.Entenberg@Einstein.yu.edu | e-mail
718.678.1116 | phone
718.678.1119 | facsimile
<http://www.aecom.yu.edu/asb> | web

December 30, 2018

Dr. Nandita Singh
Senior Science Editor, JoVE

Dear Dr. Singh,

Thank you very much for your invitation to submit our work to JoVE. In response, we are sending herewith a manuscript entitled "Assessing TMEM Doorway-Mediated Vascular Permeability Associated with Cancer Cell Dissemination, using Intravital Imaging and Fixed Tissue Analysis"

With cancer the second leading cause of mortality worldwide, the development of methods to understand its metastatic progression, particularly in response to therapeutic treatments, are of utmost importance. The methods described in our manuscript have enabled us to directly visualize and quantitate, in living animals as well as excised tumor tissue that has been formalin fixed and paraffin embedded, the transient vascular leakage that is associated with breast cancer cell intravasation and dissemination, and that is mediated by TMEM, the doorway for these cells to intravasate. We have further used these methods as bio-markers of metastatic progression during chemotherapy to determine the effect that these treatments have on creating a pro-metastatic primary tumor micro-environment that enhances breast cancer cell dissemination, as well as to determine the effect of small molecule inhibitors in abrogating these effects.

Included in this submission is the manuscript itself and two figures.

We thank you again for the invitation and for your time. We look forward to hearing from you.

Sincerely yours,

David Entenberg, Ph.D.
Senior Associate
Director of Integrated Imaging
Director of Technological Development
Einstein College of Medicine
Department of Anatomy and Structural Biology
Gruss-Lipper Biophotonics Center
and Integrated Imaging Program
1301 Morris Park Avenue, Price 202
Bronx, New York 10461
Tel: 718-678-1116; Fax: 718-678-1019
Email: david.entenberg@einstein.yu.edu

TITLE:

Assessing Tumor Microenvironment of Metastasis Doorway-Mediated Vascular Permeability Associated with Cancer Cell Dissemination using Intravital Imaging and Fixed Tissue Analysis

AUTHORS & AFFILIATIONS:

George S. Karagiannis^{1,2,3}, Jessica M. Pastoriza⁴, Lucia Borriello¹, Rojin Jafari¹, Anouchka Coste^{1,4}, John S. Condeelis^{1,2,3,4}, Maja H. Oktay^{1,2,3,5}, David Entenberg^{1,2,3}

¹Department of Anatomy and Structural Biology, Albert Einstein College of Medicine

²Gruss-Lipper Biophotonics Center, Albert Einstein College of Medicine

³Intravital Imaging Program, Albert Einstein College of Medicine

⁴Department of Surgery, Montefiore Medical Center

⁵Department of Pathology, Montefiore Medical Center

Corresponding Authors:

David Entenberg (david.entenberg@einstein.yu.edu)

George S. Karagiannis (georgios.karagiannis@einstein.yu.edu)

Maja H. Oktay (maja.oktay@einstein.yu.edu)

John S. Condeelis (john.condeelis@einstein.yu.edu)

Email Addresses of Co-Authors:

Jessica M. Pastoriza (jpastoriza05@gmail.com)

Lucia Borriello (lucia.borriello@einstein.yu.edu)

Rojin Jafari (sjafari@mail.einstein.yu.edu)

Anouchka Coste (anouchka.coste@einstein.yu.edu)

KEYWORDS:

intravital imaging, immunofluorescence, blood vessel permeability, tumor microenvironment of metastasis (TMEM), high molecular weight dextran, immunofluorescence, metastasis

SUMMARY:

We describe two methods for assessing transient vascular permeability associated with tumor microenvironment of metastasis (TMEM) doorway function and cancer cell intravasation using intravenous injection of high-molecular weight (155 kDa) dextran in mice. The methods include intravital imaging in live animals and fixed tissue analysis using immunofluorescence.

ABSTRACT:

The most common cause of cancer related mortality is metastasis, a process that requires dissemination of cancer cells from the primary tumor to secondary sites. Recently, we established that cancer cell dissemination in primary breast cancer and at metastatic sites in the lung occurs only at doorways called Tumor MicroEnvironment of Metastasis (TMEM). TMEM doorway number is prognostic for distant recurrence of metastatic disease in breast cancer patients. TMEM doorways are composed of a cancer cell which over-expresses the actin regulatory protein Mena in direct contact with a perivascular, proangiogenic macrophage which expresses high

levels of TIE2 and VEGF, where both of these cells are tightly bound to a blood vessel endothelial cell. Cancer cells can intravasate through TMEM doorways due to transient vascular permeability orchestrated by the joint activity of the TMEM-associated macrophage and the TMEM-associated Mena-expressing cancer cell. In this manuscript, we describe two methods for assessment of TMEM-mediated transient vascular permeability: intravital imaging and fixed tissue immunofluorescence. Although both methods have their advantages and disadvantages, combining the two may provide the most complete analyses of TMEM-mediated vascular permeability as well as microenvironmental prerequisites for TMEM function. Since the metastatic process in breast cancer, and possibly other types of cancer, involves cancer cell dissemination via TMEM doorways, it is essential to employ well established methods for the analysis of the TMEM doorway activity. The two methods described here provide a comprehensive approach to the analysis of TMEM doorway activity, either in naïve or pharmacologically treated animals, which is of paramount importance for pre-clinical trials of agents that prevent cancer cell dissemination via TMEM.

INTRODUCTION:

Recent advances in our understanding of cancer metastasis have uncovered that epithelial-to-mesenchymal transition (EMT) and the induction of a migratory/invasive cancer cell subpopulation are not, by themselves, sufficient for hematogenous dissemination¹. Indeed, it was previously thought that metastasizing cancer cells intravasate through the entirety of cancer-associated endothelium as the tumor neovasculature is often characterized by low pericyte coverage, and as such, is highly permeable and unstable²⁻⁴. Although highly suggestive of defective functions within the tumor, vascular modifications during carcinogenesis do not provide evidence per se that tumor cells can penetrate blood vessels easily and in an uncontrolled fashion. Insights from intravital imaging (IVI) studies, in which tumor cells are fluorescently-tagged and the vasculature is labeled via the intravenous injection of fluorescent probes (such as dextran or quantum dots), show that, while tumor vessels are uniformly permeable to low molecular weight dextrans (e.g. 70 kD), high molecular weight dextrans (155 kD) and tumor cells can cross the endothelium only at specialized sites of intravasation which are preferentially located at vascular branch points⁵⁻⁷. Immunohistochemical (IHC) analyses using animal models and human patient-derived material have shown that these sites are “doorways” that specialize in regulating vascular permeability, locally and transiently, providing a brief window of opportunity for migratory/invasive cancer cells to enter the circulation. These doorways are called “Tumor Microenvironment of Metastasis” or “TMEM”, and, quite expectedly, their density correlates with an increased risk of developing metastatic disease in breast cancer patients⁸⁻¹⁰.

Each TMEM doorway consists of three distinct types of cells: a perivascular macrophage, a tumor cell over-expressing the actin-regulatory protein mammalian enabled (Mena), and an endothelial cell, all in direct physical contact with each other^{1,5,9-13}. The key event for the function of TMEM as an intravasation doorway is the localized release of vascular endothelial growth factor (VEGF) onto the underlying vessel by the perivascular macrophage¹⁴. VEGF can disrupt homotypic junctions between endothelial cells¹⁵⁻¹⁹, a phenomenon that results in transient vascular leakage, also known as “bursting” permeability as described in IVI studies⁵. TMEM macrophages have been shown to express the tyrosine kinase receptor TIE2, which is required for VEGF-mediated

TMEM function and homing of these macrophages to the perivascular niche^{5,20-22}. In addition to regulating cancer cell dissemination and metastasis, TIE2⁺ macrophages have been shown to be central regulators of tumor angiogenesis²¹⁻³¹. As such, TIE2⁺ macrophages represent a critical constituent of the tumor microenvironment and the main regulator of the metastatic cascade.

To better conceptualize TMEM-mediated vascular permeability (i.e. “bursting”), it is very important to distinguish it from other modes of vascular permeability that are not associated with the dissolution of endothelial cell-cell junctions. In an intact endothelium (one whose tight and adherens junctions are not disrupted), there are three main types of vascular permeability: (a) pinocytosis, which may, or may not, be coupled to transcytosis of the ingested material; (b) transportation of material through endothelial fenestrae; and (c) transportation of material through the paracellular pathway, which is regulated by endothelial tight junctions^{15-19,32-34}. Although deregulated in many tumors, the aforementioned modes of vascular permeability have been described mostly in the context of normal tissue physiology and homeostasis, the extremes of which are tissues with either limited permeability (e.g., blood-brain barrier, blood-testis barrier), or abundant permeability (e.g., fenestrated capillaries of the kidney glomerular apparatus)³⁴⁻³⁷.

Using multiphoton intravital imaging and multiplexed immunofluorescence microscopy, we are able to distinguish between TMEM-mediated vascular permeability (“bursting”) and other modes of vascular permeability in breast tumors. To achieve this, we perform a single intravenous injection of a high-molecular weight, fluorescently-labeled probe in mice. Spontaneous bursting events can then be captured using intravital imaging in live mice; or alternatively, extravasation of the probe can be quantified by co-localization studies with blood vasculature (e.g. CD31⁺ or Endomucin⁺) and TMEM doorways using immunofluorescence microscopy. The protocols presented here describe both of these techniques, which could be used either independently or in conjunction with one another.

PROTOCOL:

All experiments using live animals must be conducted in accordance with animal use and care guidelines and regulations. The procedures described in this study were carried out in accordance with the National Institutes of Health regulations concerning the care and use of experimental animals and with the approval of the Albert Einstein College of Medicine Animal Care and Use Committee (IACUC).

1. Evaluation of “bursting permeability” using live animal imaging

1.1. Transplantation of syngeneic breast tumors into mouse hosts with fluorescent macrophages

1.1.1. Generate pieces of tumor tissue suitable for transplantation.

1.1.1.1. Generate fluorescently-labeled tumors in mouse mammary cancer models by crossing the spontaneous, autochthonous, genetically engineered mouse mammary cancer model MMTV-PyMT mice with transgenic mice expressing fluorescent reporters^{38,39} [e.g., enhanced green fluorescent protein (EGFP), enhanced cyan fluorescent protein (ECFP), or Dendra2].

1.1.1.2. Allow the MMTV-PyMT mice with fluorescently labeled tumors to grow to a size of no larger than 2 cm (approximately 10–12 weeks of age).

1.1.1.3. Euthanize the tumor bearing MMTV-PyMT mice by placing them into a chamber with 5% isoflurane until 30 seconds after all respirations stop.

1.1.1.4. Perform a cervical dislocation.

1.1.1.5. Remove hair from the euthanized mouse's abdomen using a topical depilatory cream.

1.1.1.6. Place a Petri dish with DMEM/F12 cell culture medium on ice.

1.1.1.7. Place the mouse and Petri dish on ice into the fume hood.

1.1.1.8. Sanitize the mouse's abdomen with 70% ethyl alcohol.

1.1.1.9. Using sterile gloves and surgical tools (sterilized scissors, forceps, and blade) remove the tumors and place them into the Petri dish.

1.1.1.10. Cut up the tumor into small pieces (~2 mm x 2 mm x 2mm in size), discarding any necrotic portions, while they are in the Petri dish.

1.1.2. Transplant the tumor pieces into recipient hosts.

1.1.2.1. Raise mice with genetically engineered fluorescently-labeled macrophages, e.g., MacGreen⁴⁰ or MacBlue⁴¹ mice (*Csf1r*-GAL4VP16/UAS-ECFP)

1.1.2.2. Allow the FVB mice with fluorescently labeled macrophages to grow to an age of ~4–6 weeks).

1.1.2.3. Anesthetize the FVB mice with fluorescently labeled macrophages in a chamber using 5% isoflurane with oxygen as a carrier gas.

1.1.2.4. Reduce the anesthesia to ~3% isoflurane and apply ophthalmic ointment to the eyes of the mouse to prevent drying.

1.1.2.5. Remove hair from over the 4th mammary gland of the mouse.

1.1.2.6. Clean the skin with betadine. It is important to maintain sterile conditions throughout the rest of the procedure. This includes using sterilized instruments and reagents.

1.1.2.7. Make a small incision ~2–3 mm just inferior to the 4th nipple.

1.1.2.8. Dissect until the mammary fat pad is exposed.

1.1.2.9. Take a tumor piece from the Petri dish and coat in artificial extracellular matrix.

1.1.2.10. Transplant tumors underneath the 4th mammary fat pad.

1.1.2.11. Close the incision using cyanoacrylate adhesive.

1.1.2.12. Continuously monitor the animal until it fully recovers from anesthesia and is able to maintain sternal recumbency. Also, do not return the animal to the company of other animals until full recovery.

1.1.2.13. Add 1 mL of enrofloxacin antibiotic to the animal's drinking water.

1.1.2.14. Allow tumors to grow until palpable (~5 mm; ~4 weeks).

1.1.2.15. Depending on the experiment, allocate the mice into treatment groups, and perform the corresponding treatments, if applicable.

1.2. Setup for intravital imaging

1.2.1. Turn on microscope's two-photon laser and detectors.

1.2.2. Turn on the heating box and pre-heat the microscope's x-y stage.

1.2.3. Place the custom-made stage insert⁴² into the x-y stage.

1.3. Preparation of imaging window

1.3.1. Prior to setting up for imaging, autoclave the custom-made circular imaging window frame⁴².

1.3.2. Use a pipette or an insulin syringe to place a thin layer of cyanoacrylate adhesive to the window frame and affix in place an 8 mm circular cover glass.

NOTE: 1) It is important to avoid getting residue on the clear aperture of the cover glass. 2) It is important to adhere the cover glass to the window frame at least 1 h before use for imaging.

1.3.3. Carefully wipe clean any excess cyanoacrylate on the clear aperture of the cover glass using a laboratory wipe wetted with a small amount of acetone.

1.4. Preparation of tail vein catheter for administration of fluids and fluorescent dyes during imaging

1.4.1. Cut a 30 cm piece of polyethylene tubing to construct a tail vein catheter.

1.4.2. Detach the needle portion of a 30 G needle from its Luer taper by gently bending the needle back and forth until it breaks.

NOTE: The needle should be held close to the Luer taper and not the needle tip. This can be performed with pliers or forceps to grasp the needle in order to prevent needle stick injury.

1.4.3. Insert the blunt end of the needle into one end of the polyethylene tubing.

1.4.4. Insert the sharp end of another 30 G needle, keeping its Luer taper attached, to the opposite end of the tubing.

1.4.5. Fill a 1 cc syringe with phosphate buffered saline, attach it to Luer taper of the assembled catheter, and flush the tail vein catheter making sure that there are no air bubbles in the system.

1.4.6. For vascular labeling, fill a 1 cc syringe with 100 μ L of 10 mg/kg 155 kDa dextran-tetramethylrhodamine (TMR) or quantum dots.

1.5. Preparation of mouse for imaging

1.5.1. Anesthetize the mouse in a cage underneath (~1 foot below) a heat lamp using 4%–5% isoflurane mixed with 100% oxygen set to a flow of 1.5–2 L per min.

1.5.2. Turn on heat lamp over surgical working area. This step is critical for maintaining the core physiologic body temperature of the mouse during the surgery.

1.5.3. Place the mouse under the heat lamp and lower the anesthesia to 2%–3% for the duration of the surgery.

NOTE: Be sure to keep the heat lamp at a safe distance (~1 foot) away from the mouse to avoid overheating.

1.5.4. Place ophthalmic ointment on the mouse's eyes to prevent drying of the eyes and blindness.

1.5.5. Test that the mouse is anesthetized by performing toe-pinch test. If animal withdraws, increase dosage of isoflurane by 1% and retest in 1–2 min.

1.5.6. Insert the tail vein catheter into the most distal point on the tail possible.

1.5.7. Affix the tail vein catheter to the tail with a small piece of lab tape that wraps around the tail and sticks to the needle to insure it does not get dislodged.

1.5.8. Inject 50 μL per h of PBS through the tail vein catheter to provide adequate hydration. It is critical to avoid injecting too much fluid (no more than 200 μL per h) or any bubbles into the catheter as this can be fatal to the mouse.

1.5.9. Remove hair on the abdomen over the 4th and 5th mammary glands using depilatory cream.

1.5.10. Clean the skin with betadine and allow skin to dry.

1.5.11. Make a longitudinal midline incision starting immediately superior to the genitals and carry the incision up to the level of the superior aspect of the 4th mammary gland.

1.5.12. Carry the incision transverse to the superior aspect of the 4th mammary gland. It is critical to avoid compromising the blood supply at this point.

1.5.13. Dissect the mammary fat pad off the peritoneum creating a tissue flap using sterile forceps and scissors.

NOTE: Skin flap imaging is susceptible to significant motion artifacts and tissue dehydration. These are avoided, as described previously^{43,44}, by affixing a rigid piece of rubber behind to the skin side of the flap (to stiffen the soft tissue and isolate it from the rest of the body) and then placing the tumor into a shallow imaging window to preserve the hydration. This is critical for stable imaging as the tumor and surrounding tissue in this setting are very compliant.

1.5.14. Stabilize the skin flap by affixing (with cyanoacrylate glue) a small piece of rigid rubber measuring 2 cm x 2 cm to the skin side of the flap. The tumor should be in the center of the area being stabilized by the rubber.

1.5.15. Keep exposed tissue hydrated with drops of PBS.

1.5.16. Apply a small film of cyanoacrylate to the outer rim of the custom-made imaging window frame.

1.5.17. Apply a small droplet of PBS (~10–20 μL) to the center of the cover glass.

1.5.18. Dry the surrounding flap tissue with a laboratory wipe. It is critical to make sure that the cyanoacrylate on the window frame does not come into contact with the PBS on the glass, as this can cause the cyanoacrylate to polymerize and set prematurely.

1.5.19. Affix the small imaging window to the tissue flap with the tumor at the center of the clear aperture.

1.5.20. Remove the heating box from the stage.

1.5.21. Transfer the anesthetized mouse and tail vein catheter to the microscope stage. Use extreme caution to ensure the tail vein catheter does not fall out.

1.5.22. Place mouse on the stage in the prone position.

1.5.23. Place the nose cone of isoflurane over the snout to ensure maintenance of anesthesia.

1.5.24. Insert the window into the bore on the custom x-y stage plate.

1.5.25. Place the heating box back onto the stage to maintain a physiological temperature.

1.5.26. Monitor the animal's vital signs by attaching a pulse oximeter probe via clip sensor to the back paw.

1.5.27. Slowly decrease isoflurane to 0.5%–1% to maintain adequate blood flow and avoid over anesthetizing the mouse.

1.6. Intravital imaging

NOTE: The imaging we describe in this section was performed on a custom-built two-laser multiphoton microscope that has been previously described^{5,39,45}. Briefly, a femtosecond laser is used to generate 90 femtosecond pulsed laser light centered at 880 nm. Fluorescence light is detected with three of the four simultaneously acquiring detectors (Blue = 447/60, Green = 520/65, and Red 580/60; central wavelength/bandwidth) after separation from the excitation light by a dichroic (Chroma, Z720DCXXR). The microscope stand contains a 25x, 1.05 NA (numerical aperture) long working distance (2 mm) objective lens. It is important to note that, while we have used a custom-built microscope, the protocol described below can be accomplished on any commercially available multiphoton microscope as well.

1.6.1. Place a drop of distilled water between the 25x, 1.05 NA microscope objective and the window's cover glass to make optical contact.

1.6.2. Use the microscope eyepiece to focus on areas with fluorescent tumor cells near to the surface of the window.

1.6.3. Find flowing blood vessels and labeled macrophages. It is critical to have flowing blood vessels to assess the dynamics of the vasculature.

1.6.4. Switch the microscope into multiphoton mode.

350
351 1.6.5. Set the upper and lower limits of a z-series, which measures approximately 50 μm .
352

353 1.6.5.1. Set the upper limit of the z-series by using the focus adjuster to move the objective to
354 the desired start location, at the most superficial position, and marking this position as zero
355 within the software by clicking on the Z position **Top** button.
356

357 1.6.5.2. Set the lower limit of the z-series moving the objective to the deepest layer (typically 50–
358 70 μm from the top for smaller tumors) and clicking the Z position **Bottom** button.
359

360 1.6.5.3. Set the z-step size to 5 μm .
361

362 1.6.6. Click the Time-Lapse panel button and set the time interval between acquisitions to at least
363 10 s to provide adequate time to replenish the water above the objective lens. This is done
364 manually with a squeeze pipette on the objective during the long time lapse.
365

366 1.6.7. Remove the syringe with PBS in the tail vein catheter and replace it with another syringe
367 containing the 155 kDa dextran-TMR (tetramethyl rhodamine).
368

369 1.6.8. Inject 100 μL of 155 kDa dextran-TMR via the tail vein catheter.
370

371 1.6.9. After injection, replace the TMR syringe with the PBS syringe.
372

373 1.6.10. Acquire a z-stack time-lapse imaging by clicking on the Z-Stack and Time-Lapse buttons,
374 then clicking on the record button.
375

376 1.6.11. Inject 50 μL of PBS every 30–45 min to maintain adequate hydration of the animal. Avoid
377 injecting more than 200 μL at time as this can cause fluid overload.
378

379 **1.7. Euthanasia** 380

381 1.7.1. Increase the isoflurane to 5% and keep the animal under 5% isoflurane with nose cone in
382 place until 30 s after respirations cease.
383

384 1.7.2. Remove the mouse from the stage.
385

386 1.7.3. Perform cervical dislocation.
387

388 **1.8. Image processing** 389

390 1.8.1. Load all images into ImageJ and format them into a 5 dimensional hyperstack (x, y, z, t, and
391 color channel).
392

1.8.2. Perform separation of spectral overlap (i.e.: GFP and CFP) and elimination of x-y drift from the hyperstacks using established methods³⁸.

1.8.3. Use the brightness and contrast adjustment to increase the white level of the blood channel so that the background signal becomes visible.

1.8.4. For each z slice, carefully inspect each movie for signs of transient vascular leakage (a “burst”). Running the movies at fast frame rates (40 fps) may aid this identification.

1.8.5. Once a burst has been identified, return the brightness for this channel to a normal level and crop the hyperstack to this region and z-slice.

2. Evaluation of extravascular dextran using fixed tissue analysis

2.1. Tumor and sample preparation

NOTE: The 2nd part of this protocol assumes that breast tumors have been harvested from an orthotopic transplantation mouse model of breast carcinoma (i.e. the MMTV-PyMT). This model could be the same as the one described in the 1st part of the protocol, although fluorescently-labeled tumors are not necessary at this point.

2.1.1. Following the termination of the experimental pipeline (i.e. drug treatments, etc.), perform a tail-vein injection of 100 µL of 10 mg/mL 155 kDa dextran-tetramethyl rhodamine, 1 h before sacrificing the mice.

2.1.2. Sacrifice the mice and harvest the breast tumors.

2.1.3. Fix tumors in 10% formalin for 48–72 h and proceed to paraffin-embedding.

2.1.4. Using a microtome, cut two 5 µm-thick sequential slides from the formalin-fixed paraffin-embedded (FFPE) tissues. One slide is used for staining the dextran, while the other will be used for performing TMEM triple-IHC, for reference.

NOTE: The TMEM triple-immunohistochemistry protocol has been described elsewhere¹⁰.

2.2. IF staining and scanning for the first of the two sequential sections

2.2.1. Submit slides to a standard de-paraffinization protocol. This includes two subsequent immersions in xylene (10 min each), followed by dehydration in serially diluted alcohol solutions (100%, 95%, 70%, and 50% EtOH in H₂O for 2 min each immersion).

2.2.2. Perform antigen retrieval by heating (close to boiling point) the sections submerged in citrate (pH 6.0-adjusted) for 20 min.

2.2.3. Let the samples cool to room temperature for 15–20 min and then wash in PBS 3x for 2 min each wash.

2.2.4. Block for 60–90 min in blocking buffer (10% FBS; 1% BSA; 0.0025% fish skin gelatin; 0.05% PBST, i.e. PBS with 0.05% Tween-20).

2.2.5. Incubate samples with a mixture of primary rat and rabbit antibodies which target Endomucin and TMR, respectively, and then wash in PBST 3x, 2 min each.

2.2.6. Incubate samples with a mixture of secondary donkey antibodies against rat IgG (conjugated to Alexa-647) and rabbit IgG (conjugated to Alexa-488), and then wash in PBST 3x 2 min each.

2.2.7. Perform a routine DAPI staining (i.e. immersion in DAPI solution for 5–6 min), mount the slides using a glycerol-free “hard” mounting medium, and store in a dark place until scanning.

2.2.8. For optimal results, scan the slides on a digital whole slide scanner.

2.3. Image Analysis

2.3.1. Capture 10 High Power Fields (HPFs) per case, using any software suitable for digital pathology.

2.3.2. Save the Endomucin (Red) and TMR (Green) channels separately as TIFF.

2.3.3. Using ImageJ, upload the TIFF files and convert them into 8-bit images.

2.3.4. Threshold the 8-bit images to the level of the negative control, and generate two binarized images, showing the Endomucin and TMR “masks”.

2.3.5. From the **Binary** tools, select **Fill Holes** on the Endomucin mask.

2.3.5.1. Generate and save the following five regions of interest: 1) The thresholded dextran image as “Dextran ROI” (ROI1), 2) the thresholded endomucin image as “Vascular ROI” (ROI2), 3) the inverted endomucin image as “Extravascular ROI” (ROI3), 4) the intersected “Extravascular ROI” and “Dextran ROI” image ($\text{ROI1} \cap \text{ROI3}$) as “Extravascular Dextran ROI” (ROI4), and 5) the entire image as “Tumor ROI” (ROI5).

2.3.6. Divide the ROI4 area by the ROI5 area and multiply by 100 to generate the percent area that the extravascular dextran covers in the entire tumor.

2.3.7. Repeat the process for 10-20 HPFs per case (depending on tissue availability) and generate an average Extravascular Dextran (% area) for each case.

REPRESENTATIVE RESULTS:

The experimental procedures described in this protocol article are briefly summarized and illustrated in **Figure 1A–C**.

To measure TMEM-mediated vascular permeability (“bursting activity”) and to reduce experimental noise from other modes of vascular permeability (i.e. transcellular and paracellular, as explained in the introduction), we performed intravenous (i.v.) injection of high molecular weight probes, such as 155 kDa Dextran, conjugated to tetramethyl rhodamine. Lower molecular weight dextrans did not distinguish the three modes of vascular permeability. Our prior experience has indicated that the systemic circulation of 155 kDa TMR-Dextran efficiently labeled the vasculature of both normal tissues, such as the mammary gland and the lungs (**Figure 2A,B**), as well as of neoplastic tissues, such as primary breast cancer and breast cancer metastases in lungs (**Figure 2C,D**). As also confirmed by prior studies^{5,46}, 155 kDa TMR-Dextran is thus a suitable probe for measuring “bursting” in both primary and secondary tumor sites. A characteristic example of peak bursting activity (dotted yellow area), using multiphoton intravital imaging in a primary MMTV-PyMT breast tumor is illustrated as a series of still images (**Figure 3A**). Bursting activity was always noted in association with a TMEM doorway (dotted white circle), characterized by the spatial juxtaposition of a Dendra2⁺ tumor cell a CFP⁺ macrophage and endothelium (**Figure 3A**). As mentioned, each TMEM doorway consists of a perivascular macrophage, a Mena overexpressing tumor cell, and an endothelial cell, all in direct physical contact with each other. While Mena has not been explicitly labeled in the mouse models used in these experiments, it has previously been shown to become overexpressed in late stage PyMT carcinoma⁴⁷. This simplifies the identification of TMEM doorways and eliminates the need to explicitly label Mena in the tumor cells.

To assess TMEM-dependent vascular permeability in fixed tissue analysis, we performed the procedure described in this protocol in mice which were transplanted with tumor chunks taken from 14-week old MMTV-PyMT donor mice. When mice reached an appropriate tumor size, they received a single i.v. dose of 155-kDa TMR-Dextran, as described in Part 2 of this protocol, and were sacrificed after 1 hour. The tumor tissues were collected and subjected to IF analysis. The endomucin fluorescent signal was used as an exclusion mask to the dextran fluorescent signal, allowing for discrimination between highly-permeable and low, or non-permeable, blood vessels (**Figure 3B**). As previously described in Karagiannis et al.⁴⁸, a sequential slide was also stained with the previously-established TMEM triple stain and aligned with the corresponding IF slide. Using this approach, we confirmed that the highly-permeable blood vessels within the breast tumor tissue have at least one associated TMEM doorway (**Figure 3B**).

FIGURE LEGENDS:

Figure 1. Summary of procedure. (A) Dendra-2 labeled invasive carcinoma of the breast (green) taken from a transgenic animal [*FVB/N-Tg(MMTV-PyMT)mul-Tg(MMTV-iCre)Jwp-Tg(loxP-stop-loxP-Pdendra2)Jwp*] and cut into small pieces. One piece is then orthotopically transplanted into another transgenic animal whose macrophages were labeled by cyan fluorescent protein (cyan) [*FVB/N-Tg(Cfms-gal4-vp16)-(UAS-eCFP)*]. The orthotopically transplanted tumor is then allowed to grow, after which the mouse is allocated to the appropriate treatment arm. (B) Once

the treatment is finished, the mouse is then taken for intravital imaging. Once anesthetized, a skin flap surgery is performed then stabilized with a rubber backing. A shallow imaging window is then affixed over the tumor. Finally, the mouse is then placed on the microscope stage where the window fits into the custom-made stage plate and the images can then be acquired. (C) Alternatively, the mouse from A is administered high molecular weight dextran and sacrificed after 1 hour. The tumor is then removed, fixed, and processed for paraffin embedding. Sections of the tissue are cut, stained for TMEM in IHC and dextran and vessels in IF, and scanned on a digital whole slide scanner. Finally, images from the two scans are aligned and individual fields of view are chosen for analysis and quantification of vascular leakage.

Figure 2. Visualization of TMR-Dextran labeled vasculature in healthy and diseased tissues. (A) Image of a healthy developing mammary gland within a transgenic animal whose vasculature is labeled by TMR-Dextran (red), mammary ductal epithelium labeled by the fluorescent protein Dendra-2 (green), and macrophages labeled by a cyan fluorescent protein (blue) [*FVB/N-Tg(loxP-stop-loxP-Pdendra2)Jwp-Tg(Cfms-gal4-vp16)-(UAS-eCFP)*]. (B) Healthy lung tissue visualized through a lung imaging window within a mouse whose vasculature is labeled by TMR-Dextran (red). Blue = SHG from collagen fibers. (C) Dendra2 labeled invasive ductal carcinoma taken from a transgenic animal [*FVB/N-Tg(MMTV-PyMT)mulxTg(MMTV-iCre)Jwp-Tg(loxP-stop-loxP-Pdendra2)Jwp*] and orthotopically transplanted into another transgenic animal whose macrophages are labeled by cyan fluorescent protein (blue) [*FVB/N-Tg(Cfms-gal4-vp16)-(UAS-eCFP)*] and vessels labeled with TMR-Dextran (red). (D) Lung metastases eight days after iv injection of tumor cells (E0771; labeled by the fluorescent protein Clover) into a transgenic animal whose macrophages are labeled by cyan fluorescent protein (cyan) [*FVB/N-Tg(Cfms-gal4-vp16)-(UAS-eCFP)*] and vasculature labeled by TMR-Dextran (red).

Figure 3. Visualization of TMEM-mediated vascular permeability using intravital imaging and fixed tissue analysis. (A) Stills from a time-lapsed intravital imaging movie of 155-kDa TMR-Dextran labeling of neo-angiogenic vessels (red) within a Dendra-2 labeled invasive carcinoma of the breast (green) taken from a transgenic animal [*FVB/N-Tg(MMTV-PyMT)mul-Tg(MMTV-iCre)Jwp-Tg(loxP-stop-loxP-Pdendra2)Jwp*] and orthotopically transplanted into another transgenic animal where the macrophages were labeled by cyan fluorescent protein (cyan) [*FVB/N-Tg(Cfms-gal4-vp16)-(UAS-eCFP)*]. The dotted yellow line denotes the outline of the transient vascular leakage area before ($t = 0'$), during ($t = 17'$) and after ($t = 52'$) the leakage (bursting) event. The dashed white circle points to a TMEM doorway, as captured in live imaging. (B) Multichannel immunofluorescence of Endomucin (first column), 155-kDa dextran-TMR (second column), their merged image along with DAPI (third column), the corresponding thresholded blood vessel and extravascular dextran masks (fourth column), and the corresponding sequential section of TMEM IHC (fifth column) in MMTV-PyMT mice. Top row: Vascular profile away from TMEM, appearing as a “non-leaky” vascular profile. Bottom row: TMEM-associated vascular profile, appearing as a “leaky” vascular profile.

DISCUSSION:

Here, we outline two protocols that can be applied to visualize and quantify a specific type of vascular permeability which is present at TMEM doorways and is associated with the disruption

of vascular tight and adherens junctions. This type of vascular permeability is transient and controlled by the tripartite TMEM cell complex, as explained above⁵. The ability to identify and quantify TMEM-associated vascular permeability is crucial for the assessment of a pro-metastatic cancer cell microenvironment, as well as for pre-clinical studies that examine the effect of conventional cytotoxic therapies on tumor microenvironment as well as anti-metastatic potential of targeted and non-targeted therapies. Importantly, we demonstrated here that this assessment can be done by either intravital imaging or immunofluorescence in fixed tissues. Both approaches have their advantages and disadvantages. Intravital imaging allows direct visualization of the dynamic process of vascular permeability, but requires specialized equipment and training. On the other hand, immunofluorescence performed in fixed tissues offers only a static image, but can be routinely performed in most laboratories.

Cancer patients are commonly treated with some form of systemic therapy, and the success of systemic treatment is usually assessed by the evaluation of parameters related to cancer cell survival such as apoptosis, proliferation, or gross tumor size. However, it is equally important to understand how these systemic therapies affect cancer cell dissemination given that most cancer related mortality occurs due to metastasis, a process which involves both cancer cell proliferation as well as cancer cell dissemination¹. For example, recent studies have demonstrated that chemotherapy can induce a significant increase in the density of TMEM doorways in mouse and human breast cancer^{48,49}. Moreover, it was shown that chemotherapy also induces TMEM activity and results in hematogenous dissemination of cancer cells, increased circulating cancer cells, and increased lung metastasis⁴⁸. The chemotherapy-induced increase in TMEM activity can be blocked by systemic administration of drug that inhibits TIE2 function and therefore TMEM activity, called rebastinib^{14,48}. Thus, the protocols described here can offer valuable endpoint measurements for the effect of various systemic treatments on the activity of TMEM through the comparison of treated to non-treated cohorts of mice.

In recent years, the concept of antiangiogenic therapy in cancer has been revisited, suggesting that a vascular “normalization” strategy (i.e. the transient reconstitution of the abnormal structure and function of blood vessels), may be preferable to targeting blood vessels for destruction, as it makes the neovasculature more effective for drug delivery⁵⁰⁻⁵⁴. In view of this emerging hypothesis, other groups have also developed assays for assessing vascular permeability and for testing the efficiency of vascular normalization strategies⁵⁵. It should be mentioned that, in principle, these methods are utilized to assess TMEM-independent modes of vascular permeability. Therefore, the selection of the most appropriate vascular permeability assay depends on the scope of a study, and researchers must ensure that they comprehend the applicability of each of the published vascular permeability assays, before applying them to their studies.

As mentioned above, each of the two methods described here has certain advantages over the other. For example, measuring “bursting permeability” in vivo offers valuable kinetic information, but since bursting is a rare event, prolonged imaging sessions of several hours each may be required to be able to obtain sufficient data. In addition, intravital imaging requires specialized equipment which may not be available to all investigators. On the other hand, evaluation of TMEM

activity in fixed tissues is relatively easy to perform and requires only standard laboratory equipment. In addition, the analysis of TMEM activity in fixed tissues is easier to interpret, but lacks kinetic information. Moreover, the fixed tissue analysis is less specific, since it may capture cumulative leakage of dextran over time from transcellular and paracellular vascular permeability of intact endothelia, or even a sudden leakage event due to spontaneous vascular injury. Thus, the synergistic use of the two methods would make the interpretation of the TMEM-mediated vascular permeability more specific and more sensitive. While we have not explicitly tested other applications of the techniques presented here, they may prove useful for investigating induced vessel permeability, for example by infection or by pharmaceutical therapies.

In summary, the measurement of TMEM-associated vascular permeability, as outlined by two independent methodologies here, provide useful tools for assessing the pro-metastatic tumor microenvironment and its associated TMEM activity, and can be used to some extent by any laboratory. These methods are particularly useful in the pre-clinical assessment of the effect of systemic therapies on cancer cell dissemination. In addition, they can be used to assess the effect of agents that can block chemotherapy-induced TMEM activity, and lastly, these methods can be used to assess the best combination therapy preceding phase I patient trials.

ACKNOWLEDGEMENTS:

We would like to thank the Analytical Imaging Facility (AIF) in the Albert Einstein College of Medicine for imaging support. This work was supported by grants from the NCI (P30CA013330, CA150344, CA 100324 and CA216248), the SIG 1S100D019961-01, the Gruss-Lipper Biophotonics Center and its Integrated Imaging Program, and Montefiore's Ruth L. Kirschstein T32 Training Grant of Surgeons for the Study of the Tumor Microenvironment (CA200561).

GSK co-wrote the manuscript, prepared figure 2B, developed fixed tissue analysis protocol, and analyzed and interpreted all data; **JMP** co-wrote the manuscript, and prepared Figure 1C and 2A; **LB & AC** provided Figure 1B; **RJ** provided Figure 1A; **DE** provided Figure 1D; **JSC** co-wrote the manuscript and analyzed and interpreted all data; **MHO** co-wrote the manuscript and analyzed and interpreted all data; and **DE** co-wrote the manuscript, developed fixed tissue analysis protocol and intravital imaging protocol, prepared Figures 1 & 2, and analyzed and interpreted all data.

DISCLOSURES:

The authors disclose no conflicts of interest.

REFERENCES:

- 1 Karagiannis, G. S., Goswami, S., Jones, J. G., Oktay, M. H., Condeelis, J. S. Signatures of breast cancer metastasis at a glance. *Journal of Cell Science*. **129** (9), 1751-1758, doi:10.1242/jcs.183129 (2016).
- 2 Hanahan, D., Weinberg, R. A. Hallmarks of cancer: the next generation. *Cell*. **144** (5), 646-674, doi:10.1016/j.cell.2011.02.013 (2011).

655 3 Raza, A., Franklin, M. J., Dudek, A. Z. Pericytes and vessel maturation during tumor
656 angiogenesis and metastasis. *American Journal of Hematology*. **85** (8), 593-598,
657 doi:10.1002/ajh.21745 (2010).

658 4 Pietras, K., Ostman, A. Hallmarks of cancer: interactions with the tumor stroma. *Experimental*
659 *Cell Research*. **316** (8), 1324-1331, doi:10.1016/j.yexcr.2010.02.045 (2010).

660 5 Harney, A. S. et al. Real-Time Imaging Reveals Local, Transient Vascular Permeability, and
661 Tumor Cell Intravasation Stimulated by TIE2hi Macrophage-Derived VEGFA. *Cancer Discovery*.
662 **5** (9), 932-943, doi:10.1158/2159-8290.CD-15-0012 (2015).

663 6 Kedrin, D. et al. Intravital imaging of metastatic behavior through a mammary imaging
664 window. *Nature Methods*. **5** (12), 1019-1021, doi:10.1038/nmeth.1269 (2008).

665 7 Wyckoff, J. B. et al. Direct visualization of macrophage-assisted tumor cell intravasation in
666 mammary tumors. *Cancer Research*. **67** (6), 2649-2656, doi:10.1158/0008-5472.CAN-06-1823
667 (2007).

668 8 Sparano, J. A. et al. A metastasis biomarker (MetaSite Breast Score) is associated with distant
669 recurrence in hormone receptor-positive, HER2-negative early-stage breast cancer. *npj*
670 *Breast Cancer*. **3**, 42, doi:10.1038/s41523-017-0043-5 (2017).

671 9 Rohan, T. E. et al. Tumor microenvironment of metastasis and risk of distant metastasis of
672 breast cancer. *Journal of the National Cancer Institute*. **106** (8), doi:10.1093/jnci/dju136
673 (2014).

674 10 Robinson, B. D. et al. Tumor microenvironment of metastasis in human breast carcinoma: a
675 potential prognostic marker linked to hematogenous dissemination. *Clinical Cancer Research*.
676 **15** (7), 2433-2441, doi:10.1158/1078-0432.CCR-08-2179 (2009).

677 11 Pignatelli, J. et al. Invasive breast carcinoma cells from patients exhibit MenaINV- and
678 macrophage-dependent transendothelial migration. *Science Signaling*. **7** (353), ra112,
679 doi:10.1126/scisignal.2005329 (2014).

680 12 Oktay, M. H., Jones, J. G. TMEM: a novel breast cancer dissemination marker for the
681 assessment of metastatic risk. *Biomarkers in Medicine*. **9** (2), 81-84, doi:10.2217/bmm.14.104
682 (2015).

683 13 Roussos, E. T. et al. Mena invasive (Mena(INV)) and Mena11a isoforms play distinct roles in
684 breast cancer cell cohesion and association with TMEM. *Clinical & Experimental Metastasis*.
685 **28** (6), 515-527, doi:10.1007/s10585-011-9388-6 (2011).

686 14 Harney, A. S. et al. The Selective Tie2 Inhibitor Rebastinib Blocks Recruitment and Function of
687 Tie2(Hi) Macrophages in Breast Cancer and Pancreatic Neuroendocrine Tumors. *Molecular*
688 *Cancer Therapeutics*. **16** (11), 2486-2501, doi:10.1158/1535-7163.MCT-17-0241 (2017).

689 15 Bates, D. O., Lodwick, D., Williams, B. Vascular endothelial growth factor and microvascular
690 permeability. *Microcirculation*. **6** (2), 83-96 (1999).

691 16 Lee, Y. C. The involvement of VEGF in endothelial permeability: a target for anti-inflammatory
692 therapy. *Current Opinion in Investigational Drugs*. **6** (11), 1124-1130 (2005).

693 17 Roberts, W. G., Palade, G. E. Neovasculature induced by vascular endothelial growth factor is
694 fenestrated. *Cancer Research*. **57** (4), 765-772 (1997).

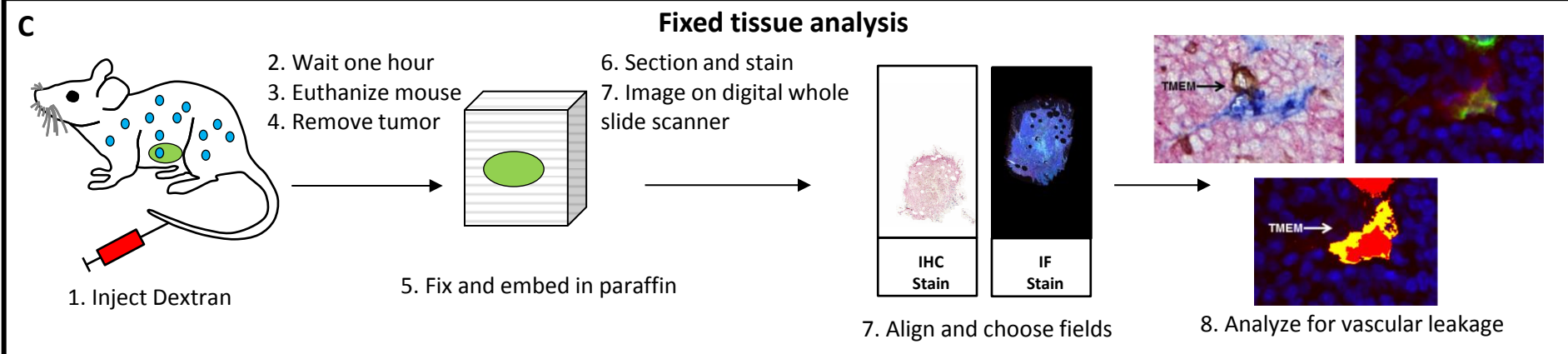
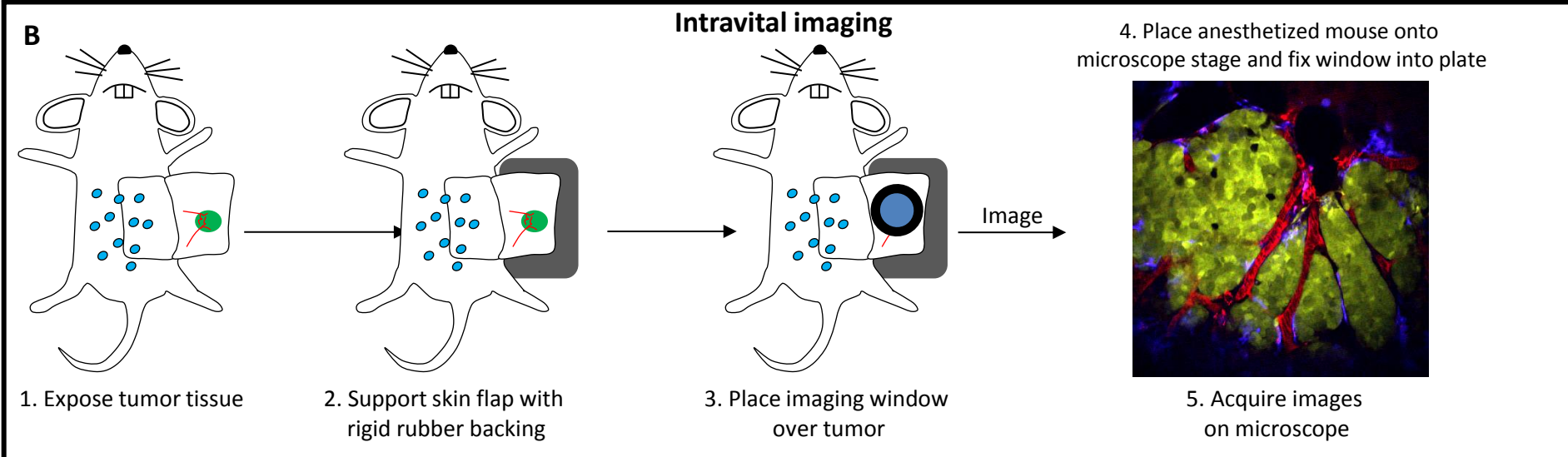
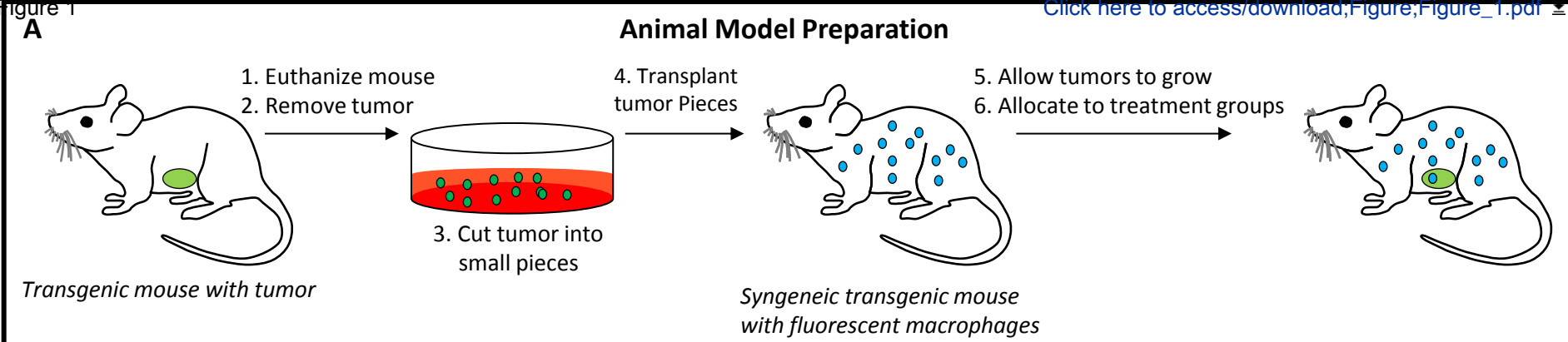
695 18 Stan, R. V. et al. Immunoisolation and partial characterization of endothelial plasmalemmal
696 vesicles (caveolae). *Molecular Biology of the Cell*. **8** (4), 595-605 (1997).

- 19 Roberts, W. G., Palade, G. E. Increased microvascular permeability and endothelial fenestration induced by vascular endothelial growth factor. *Journal of Cell Science*. **108** (Pt 6), 2369-2379 (1995).
- 20 Arwert, E. N. et al. A Unidirectional Transition from Migratory to Perivascular Macrophage Is Required for Tumor Cell Intravasation. *Cell Reports*. **23** (5), 1239-1248, doi:10.1016/j.celrep.2018.04.007 (2018).
- 21 Kadioglu, E., De Palma, M. Cancer Metastasis: Perivascular Macrophages Under Watch. *Cancer Discovery*. **5** (9), 906-908, doi:10.1158/2159-8290.CD-15-0819 (2015).
- 22 Hughes, R. et al. Perivascular M2 Macrophages Stimulate Tumor Relapse after Chemotherapy. *Cancer Research*. **75** (17), 3479-3491, doi:10.1158/0008-5472.CAN-14-3587 (2015).
- 23 Riabov, V. et al. Role of tumor associated macrophages in tumor angiogenesis and lymphangiogenesis. *Frontiers in Physiology*. **5**, 75, doi:10.3389/fphys.2014.00075 (2014).
- 24 Squadrito, M. L., De Palma, M. Macrophage regulation of tumor angiogenesis: implications for cancer therapy. *Molecular Aspects of Medicine*. **32** (2), 123-145, doi:10.1016/j.mam.2011.04.005 (2011).
- 25 Ferrara, N. Role of myeloid cells in vascular endothelial growth factor-independent tumor angiogenesis. *Current Opinion in Hematology*. **17** (3), 219-224, doi:10.1097/MOH.0b013e3283386660 (2010).
- 26 Solinas, G., Germano, G., Mantovani, A., Allavena, P. Tumor-associated macrophages (TAM) as major players of the cancer-related inflammation. *Journal of Leukocyte Biology*. **86** (5), 1065-1073, doi:10.1189/jlb.0609385 (2009).
- 27 Venneri, M. A. et al. Identification of proangiogenic TIE2-expressing monocytes (TEMs) in human peripheral blood and cancer. *Blood*. **109** (12), 5276-5285, doi:10.1182/blood-2006-10-053504 (2007).
- 28 Lewis, C. E., De Palma, M., Naldini, L. Tie2-expressing monocytes and tumor angiogenesis: regulation by hypoxia and angiopoietin-2. *Cancer Research*. **67** (18), 8429-8432, doi:10.1158/0008-5472.CAN-07-1684 (2007).
- 29 Mazzei, R. et al. Targeting the ANG2/TIE2 axis inhibits tumor growth and metastasis by impairing angiogenesis and disabling rebounds of proangiogenic myeloid cells. *Cancer Cell*. **19** (4), 512-526, doi:10.1016/j.ccr.2011.02.005 (2011).
- 30 Lewis, C. E., Ferrara, N. Multiple effects of angiopoietin-2 blockade on tumors. *Cancer Cell*. **19** (4), 431-433, doi:10.1016/j.ccr.2011.03.016 (2011).
- 31 Gabrusiewicz, K. et al. Anti-vascular endothelial growth factor therapy-induced glioma invasion is associated with accumulation of Tie2-expressing monocytes. *Oncotarget*. **5** (8), 2208-2220, doi:10.18632/oncotarget.1893 (2014).
- 32 Karagiannis, G. S., Condeelis, J. S., Oktay, M. H. Chemotherapy-induced metastasis: mechanisms and translational opportunities. *Clinical & Experimental Metastasis*. doi:10.1007/s10585-017-9870-x (2018).
- 33 Senger, D. R. et al. Tumor cells secrete a vascular permeability factor that promotes accumulation of ascites fluid. *Science*. **219** (4587), 983-985 (1983).
- 34 Obermeier, B., Verma, A., Ransohoff, R. M. The blood-brain barrier. *Handbook of Clinical Neurology*. **133**, 39-59, doi:10.1016/B978-0-444-63432-0.00003-7 (2016).

- 35 Satchell, S. C., Braet, F. Glomerular endothelial cell fenestrations: an integral component of the glomerular filtration barrier. *American Journal of Physiology: Renal Physiology*. **296** (5), F947-956, doi:10.1152/ajprenal.90601.2008 (2009).
- 36 Stan, R. V. Endothelial stomatal and fenestral diaphragms in normal vessels and angiogenesis. *Journal of Cellular and Molecular Medicine*. **11** (4), 621-643, doi:10.1111/j.1582-4934.2007.00075.x (2007).
- 37 Mruk, D. D., Cheng, C. Y. The Mammalian Blood-Testis Barrier: Its Biology and Regulation. *Endocrine Reviews*. **36** (5), 564-591, doi:10.1210/er.2014-1101 (2015).
- 38 Entenberg, D. et al. Imaging Tumor Cell Movement in Vivo. *Current Protocols in Cell Biology*. **58** (1), 19.7.1-19.7.19 (2013).
- 39 Entenberg, D. et al. Setup and use of a two-laser multiphoton microscope for multichannel intravital fluorescence imaging. *Nature Protocols*. **6** (10), 1500-1520, doi:10.1038/nprot.2011.376 (2011).
- 40 Sasmono, R. T. et al. A macrophage colony-stimulating factor receptor-green fluorescent protein transgene is expressed throughout the mononuclear phagocyte system of the mouse. *Blood*. **101** (3), 1155-1163, doi:DOI 10.1182/blood-2002-02-1569 (2003).
- 41 Ovchinnikov, D. A. et al. Expression of Gal4-dependent transgenes in cells of the mononuclear phagocyte system labeled with enhanced cyan fluorescent protein using Csf1r-Gal4VP16/UAS-ECFP double-transgenic mice. *Journal of Leukocyte Biology*. **83** (2), 430-433, doi:10.1189/jlb.0807585 (2008).
- 42 Entenberg, D. et al. Time-lapsed, large-volume, high-resolution intravital imaging for tissue-wide analysis of single cell dynamics. *Methods*. **128**, 65-77, doi:10.1016/j.ymeth.2017.07.019 (2017).
- 43 Pastoriza, J. M. et al. Black race and distant recurrence after neoadjuvant or adjuvant chemotherapy in breast cancer. *Clinical & Experimental Metastasis*. doi:10.1007/s10585-018-9932-8 (2018).
- 44 Williams, J. K. et al. Validation of a device for the active manipulation of the tumor microenvironment during intravital imaging. *Intravital*. **5** (2), e1182271, doi:10.1080/21659087.2016.1182271 (2016).
- 45 Harney, A. S., Wang, Y., Condeelis, J. S., Entenberg, D. Extended Time-lapse Intravital Imaging of Real-time Multicellular Dynamics in the Tumor Microenvironment. *Journal of Visualized Experiments*. (112), e54042, doi:10.3791/54042 (2016).
- 46 Entenberg, D. et al. A permanent window for the murine lung enables high-resolution imaging of cancer metastasis. *Nature Methods*. **15** (1), 73-80, doi:10.1038/nmeth.4511 (2018).
- 47 Roussos, E. T. et al. Mena invasive (MenaINV) promotes multicellular streaming motility and transendothelial migration in a mouse model of breast cancer. *Journal of Cell Science*. **124** (Pt 13), 2120-2131, doi:10.1242/jcs.086231 (2011).
- 48 Karagiannis, G. S. et al. Neoadjuvant chemotherapy induces breast cancer metastasis through a TMEM-mediated mechanism. *Science Translational Medicine*. **9** (397), doi:10.1126/scitranslmed.aan0026 (2017).
- 49 Chang, Y. S., Jalgaonkar, S. P., Middleton, J. D., Hai, T. Stress-inducible gene Atf3 in the noncancer host cells contributes to chemotherapy-exacerbated breast cancer metastasis. *Proceedings of the National Academy of Sciences of the United States of America*. **114** (34), E7159-E7168, doi:10.1073/pnas.1700455114 (2017).

- 784 50 Jain, R. K. Normalization of tumor vasculature: an emerging concept in antiangiogenic
785 therapy. *Science*. **307** (5706), 58-62, doi:10.1126/science.1104819 (2005).
- 786 51 Winkler, F. et al. Kinetics of vascular normalization by VEGFR2 blockade governs brain tumor
787 response to radiation: role of oxygenation, angiopoietin-1, and matrix metalloproteinases.
788 *Cancer Cell*. **6** (6), 553-563, doi:10.1016/j.ccr.2004.10.011 (2004).
- 789 52 Goel, S. et al. Normalization of the vasculature for treatment of cancer and other diseases.
790 *Physiological Reviews*. **91** (3), 1071-1121, doi:10.1152/physrev.00038.2010 (2011).
- 791 53 Jain, R. K. Normalizing tumor microenvironment to treat cancer: bench to bedside to
792 biomarkers. *Journal of Clinical Oncology*. **31** (17), 2205-2218, doi:10.1200/JCO.2012.46.3653
793 (2013).
- 794 54 Carmeliet, P., Jain, R. K. Principles and mechanisms of vessel normalization for cancer and
795 other angiogenic diseases. *Nature Reviews Drug Discovery*. **10** (6), 417-427,
796 doi:10.1038/nrd3455 (2011).
- 797 55 Meijer, E. F., Baish, J. W., Padera, T. P., Fukumura, D. Measuring Vascular Permeability In Vivo.
798 *Methods in Molecular Biology*. **1458**, 71-85, doi:10.1007/978-1-4939-3801-8_6 (2016).

799



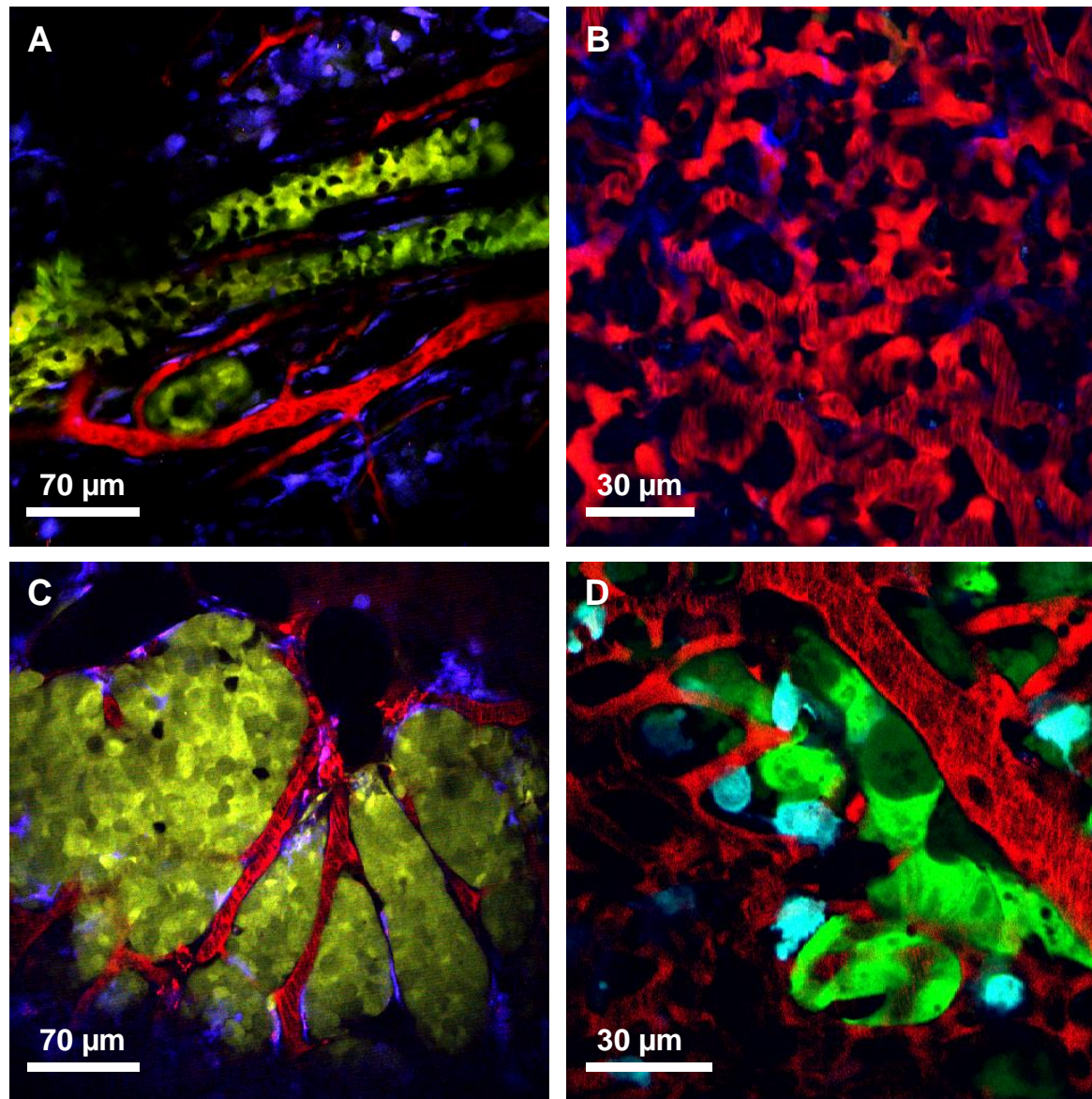
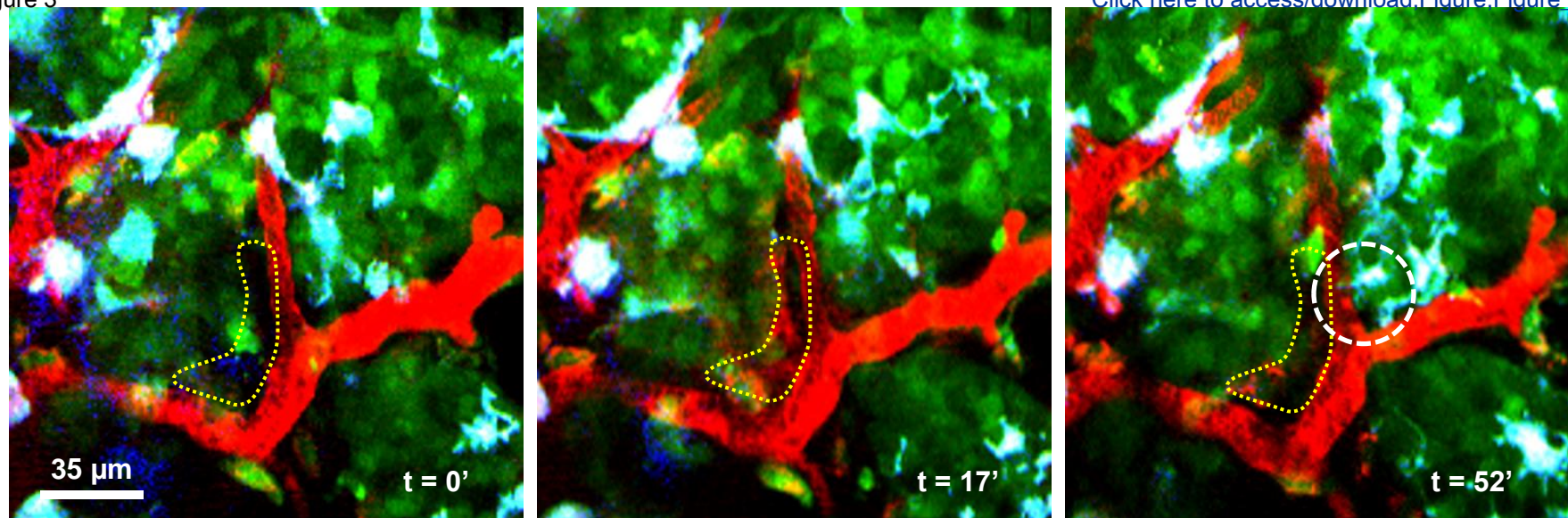
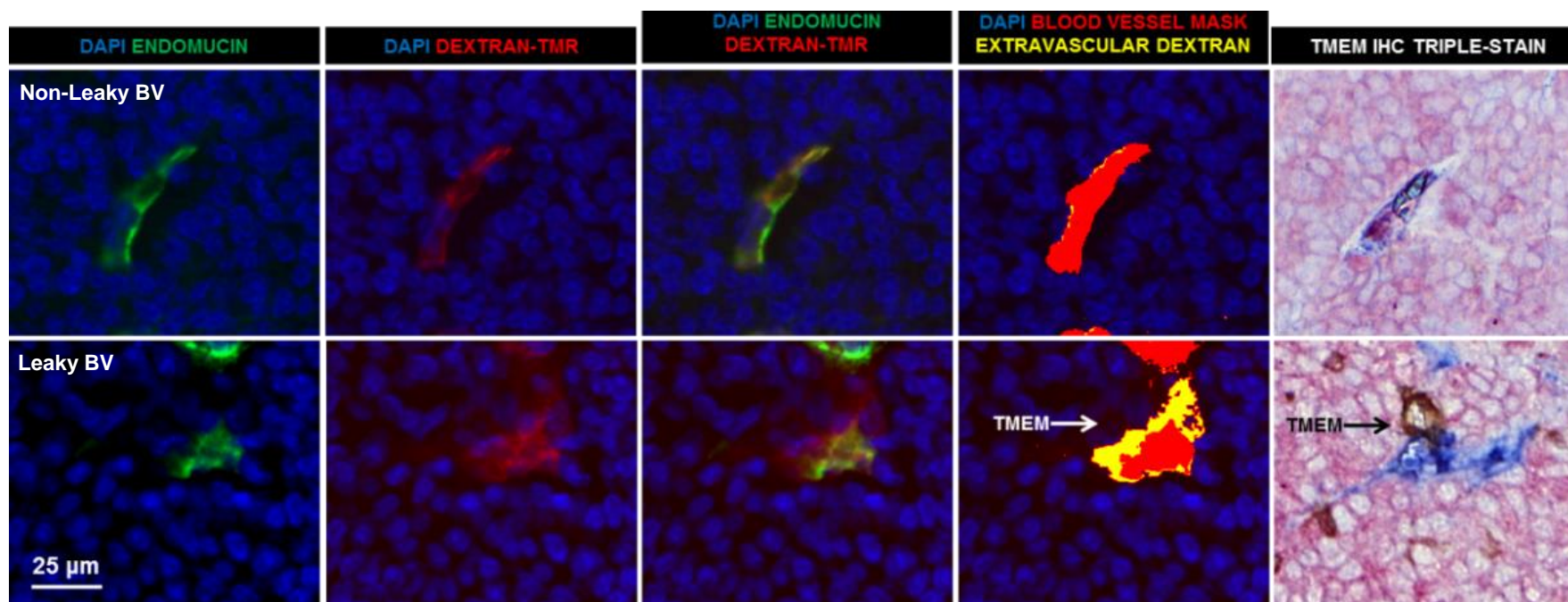


Figure 3

[Click here to access/download:Figure:Figure_3.pdf](#)



B



Reagent	Company	Catalogue Number
Anti-rabbit IgG (Alexa 488)	Life Technologies Corporation	A-11034
Anti-rat IgG (Alexa 647)	Life Technologies Corporation	A-21247
Bovine Serum Albumin	Fisher Scientific	BP1600-100
Citrate	Eng Scientific Inc	9770
Cover Glass Slips	Electron Microscopy Sciences	72296-08
Cyanoacrylate Adhesive	Henkel Adhesive	1647358
DAPI	Perkin Elmer	FP1490
Dextran-Tetramethyl-Rhodamine	Sigma Aldrich	T1287
DMEM/F12	Gibco	11320-033
Endomucin (primary antibody)	Santa Cruz Biotechnology	sc-65495
Enrofloxacin	Bayer	84753076 v-06/2015
Fetal Bovine Serum	Sigma Aldrich	F2442
Fish Skin Gelatin	Fisher Scientific	G7765
Insulin Syringe	Becton Dickinson	309659
Isofluorane	Henry Schein	NDC 11695-6776-2
Matrigel	Corning	CB40234
Needle (30 G)	Becton Dickinson	305128
Phosphate Buffered Saline	Life Technologies Corporation	PBS
Polyethylene Tubing	Scientific Commodities Inc	BB31695-PE/1
Pulse Oximeter	Kent Scientific	MouseOx
Puralube Vet Ointment	Dechra	NDC 17033-211-38
Quantum Dots	Life Technologies Corporation	Q21561MP
Rubber	McMaster Carr	1310N14
TMR (primary antibody)	Invitrogen	A6397
Tween-20	MP Biologicals	TWEEN201
Xylene	Fisher Scientific	184835

Artificial extracellular matrix



1 Alewife Center #200
Cambridge, MA 02140
tel. 617.945.9051
www.jove.com

ARTICLE AND VIDEO LICENSE AGREEMENT

Title of Article: Analysis of Tmem-40-mediated Transient Vascular Permeability Associated with Breast Cancer Cell Dissemination, using Intravital Imaging and Fixed Tissue Analysis

Author(s): Konstantinos G.S. Pastoriza JM, Bottiello L, Jofari R, Coste A, Condeelis JS, Ostuy MH, Entenber D.

Item 1: The Author elects to have the Materials be made available (as described at <http://www.jove.com/publish>) via:



Standard Access



Open Access

Item 2: Please select one of the following items:



The Author is **NOT** a United States government employee.



The Author is a United States government employee and the Materials were prepared in the course of his or her duties as a United States government employee.



The Author is a United States government employee but the Materials were NOT prepared in the course of his or her duties as a United States government employee.

ARTICLE AND VIDEO LICENSE AGREEMENT

1. **Defined Terms.** As used in this Article and Video License Agreement, the following terms shall have the following meanings: **"Agreement"** means this Article and Video License Agreement; **"Article"** means the article specified on the last page of this Agreement, including any associated materials such as texts, figures, tables, artwork, abstracts, or summaries contained therein; **"Author"** means the author who is a signatory to this Agreement; **"Collective Work"** means a work, such as a periodical issue, anthology or encyclopedia, in which the Materials in their entirety in unmodified form, along with a number of other contributions, constituting separate and independent works in themselves, are assembled into a collective whole; **"CRC License"** means the Creative Commons Attribution-Non Commercial-No Derivs 3.0 Unported Agreement, the terms and conditions of which can be found at: <http://creativecommons.org/licenses/by-nc-nd/3.0/legalcode>; **"Derivative Work"** means a work based upon the Materials or upon the Materials and other pre-existing works, such as a translation, musical arrangement, dramatization, fictionalization, motion picture version, sound recording, art reproduction, abridgment, condensation, or any other form in which the Materials may be recast, transformed, or adapted; **"Institution"** means the institution, listed on the last page of this Agreement, by which the Author was employed at the time of the creation of the Materials; **"JoVE"** means MyJoVE Corporation, a Massachusetts corporation and the publisher of The Journal of Visualized Experiments; **"Materials"** means the Article and / or the Video; **"Parties"** means the Author and JoVE; **"Video"** means any video(s) made by the Author, alone or in conjunction with any other parties, or by JoVE or its affiliates or agents, individually or in collaboration with the Author or any other parties, incorporating all or any portion

of the Article, and in which the Author may or may not appear.

2. **Background.** The Author, who is the author of the Article, in order to ensure the dissemination and protection of the Article, desires to have the JoVE publish the Article and create and transmit videos based on the Article. In furtherance of such goals, the Parties desire to memorialize in this Agreement the respective rights of each Party in and to the Article and the Video.

3. **Grant of Rights in Article.** In consideration of JoVE agreeing to publish the Article, the Author hereby grants to JoVE, subject to **Sections 4 and 7** below, the exclusive, royalty-free, perpetual (for the full term of copyright in the Article, including any extensions thereto) license (a) to publish, reproduce, distribute, display and store the Article in all forms, formats and media whether now known or hereafter developed (including without limitation in print, digital and electronic form) throughout the world, (b) to translate the Article into other languages, create adaptations, summaries or extracts of the Article or other Derivative Works (including, without limitation, the Video) or Collective Works based on all or any portion of the Article and exercise all of the rights set forth in (a) above in such translations, adaptations, summaries, extracts, Derivative Works or Collective Works and (c) to license others to do any or all of the above. The foregoing rights may be exercised in all media and formats, whether now known or hereafter devised, and include the right to make such modifications as are technically necessary to exercise the rights in other media and formats. If the "Open Access" box has been checked in **Item 1** above, JoVE and the Author hereby grant to the public all such rights in the Article as provided in, but subject to all limitations and requirements set forth in, the CRC License.

ARTICLE AND VIDEO LICENSE AGREEMENT

4. **Retention of Rights in Article.** Notwithstanding the exclusive license granted to JoVE in **Section 3** above, the Author shall, with respect to the Article, retain the non-exclusive right to use all or part of the Article for the non-commercial purpose of giving lectures, presentations or teaching classes, and to post a copy of the Article on the Institution's website or the Author's personal website, in each case provided that a link to the Article on the JoVE website is provided and notice of JoVE's copyright in the Article is included. All non-copyright intellectual property rights in and to the Article, such as patent rights, shall remain with the Author.

5. **Grant of Rights in Video – Standard Access.** This **Section 5** applies if the "Standard Access" box has been checked in **Item 1** above or if no box has been checked in **Item 1** above. In consideration of JoVE agreeing to produce, display or otherwise assist with the Video, the Author hereby acknowledges and agrees that, Subject to **Section 7** below, JoVE is and shall be the sole and exclusive owner of all rights of any nature, including, without limitation, all copyrights, in and to the Video. To the extent that, by law, the Author is deemed, now or at any time in the future, to have any rights of any nature in or to the Video, the Author hereby disclaims all such rights and transfers all such rights to JoVE.

6. **Grant of Rights in Video – Open Access.** This **Section 6** applies only if the "Open Access" box has been checked in **Item 1** above. In consideration of JoVE agreeing to produce, display or otherwise assist with the Video, the Author hereby grants to JoVE, subject to **Section 7** below, the exclusive, royalty-free, perpetual (for the full term of copyright in the Article, including any extensions thereto) license (a) to publish, reproduce, distribute, display and store the Video in all forms, formats and media whether now known or hereafter developed (including without limitation in print, digital and electronic form) throughout the world, (b) to translate the Video into other languages, create adaptations, summaries or extracts of the Video or other Derivative Works or Collective Works based on all or any portion of the Video and exercise all of the rights set forth in (a) above in such translations, adaptations, summaries, extracts, Derivative Works or Collective Works and (c) to license others to do any or all of the above. The foregoing rights may be exercised in all media and formats, whether now known or hereafter devised, and include the right to make such modifications as are technically necessary to exercise the rights in other media and formats. For any Video to which this **Section 6** is applicable, JoVE and the Author hereby grant to the public all such rights in the Video as provided in, but subject to all limitations and requirements set forth in, the CRC License.

7. **Government Employees.** If the Author is a United States government employee and the Article was prepared in the course of his or her duties as a United States government employee, as indicated in **Item 2** above, and any of the licenses or grants granted by the Author hereunder exceed the scope of the 17 U.S.C. 403, then the rights granted hereunder shall be limited to the maximum

rights permitted under such statute. In such case, all provisions contained herein that are not in conflict with such statute shall remain in full force and effect, and all provisions contained herein that do so conflict shall be deemed to be amended so as to provide to JoVE the maximum rights permissible within such statute.

8. **Protection of the Work.** The Author(s) authorize JoVE to take steps in the Author(s) name and on their behalf if JoVE believes some third party could be infringing or might infringe the copyright of either the Author's Article and/or Video.

9. **Likeness, Privacy, Personality.** The Author hereby grants JoVE the right to use the Author's name, voice, likeness, picture, photograph, image, biography and performance in any way, commercial or otherwise, in connection with the Materials and the sale, promotion and distribution thereof. The Author hereby waives any and all rights he or she may have, relating to his or her appearance in the Video or otherwise relating to the Materials, under all applicable privacy, likeness, personality or similar laws.

10. **Author Warranties.** The Author represents and warrants that the Article is original, that it has not been published, that the copyright interest is owned by the Author (or, if more than one author is listed at the beginning of this Agreement, by such authors collectively) and has not been assigned, licensed, or otherwise transferred to any other party. The Author represents and warrants that the author(s) listed at the top of this Agreement are the only authors of the Materials. If more than one author is listed at the top of this Agreement and if any such author has not entered into a separate Article and Video License Agreement with JoVE relating to the Materials, the Author represents and warrants that the Author has been authorized by each of the other such authors to execute this Agreement on his or her behalf and to bind him or her with respect to the terms of this Agreement as if each of them had been a party hereto as an Author. The Author warrants that the use, reproduction, distribution, public or private performance or display, and/or modification of all or any portion of the Materials does not and will not violate, infringe and/or misappropriate the patent, trademark, intellectual property or other rights of any third party. The Author represents and warrants that it has and will continue to comply with all government, institutional and other regulations, including, without limitation all institutional, laboratory, hospital, ethical, human and animal treatment, privacy, and all other rules, regulations, laws, procedures or guidelines, applicable to the Materials, and that all research involving human and animal subjects has been approved by the Author's relevant institutional review board.

11. **JoVE Discretion.** If the Author requests the assistance of JoVE in producing the Video in the Author's facility, the Author shall ensure that the presence of JoVE employees, agents or independent contractors is in accordance with the relevant regulations of the Author's institution. If more than one author is listed at the beginning of this Agreement, JoVE may, in its sole

ARTICLE AND VIDEO LICENSE AGREEMENT

discretion, elect not take any action with respect to the Article until such time as it has received complete, executed Article and Video License Agreements from each such author. JoVE reserves the right, in its absolute and sole discretion and without giving any reason therefore, to accept or decline any work submitted to JoVE. JoVE and its employees, agents and independent contractors shall have full, unfettered access to the facilities of the Author or of the Author's institution as necessary to make the Video, whether actually published or not. JoVE has sole discretion as to the method of making and publishing the Materials, including, without limitation, to all decisions regarding editing, lighting, filming, timing of publication, if any, length, quality, content and the like.

12. **Indemnification.** The Author agrees to indemnify JoVE and/or its successors and assigns from and against any and all claims, costs, and expenses, including attorney's fees, arising out of any breach of any warranty or other representations contained herein. The Author further agrees to indemnify and hold harmless JoVE from and against any and all claims, costs, and expenses, including attorney's fees, resulting from the breach by the Author of any representation or warranty contained herein or from allegations or instances of violation of intellectual property rights, damage to the Author's or the Author's institution's facilities, fraud, libel, defamation, research, equipment, experiments, property damage, personal injury, violations of institutional, laboratory, hospital, ethical, human and animal treatment, privacy or other rules, regulations, laws, procedures or guidelines, liabilities and other losses or damages related in any way to the submission of work to JoVE, making of videos by JoVE, or publication in JoVE or elsewhere by JoVE. The Author shall be responsible for, and shall hold JoVE harmless from, damages caused by lack of sterilization, lack of cleanliness or by contamination due to

the making of a video by JoVE its employees, agents or independent contractors. All sterilization, cleanliness or decontamination procedures shall be solely the responsibility of the Author and shall be undertaken at the Author's expense. All indemnifications provided herein shall include JoVE's attorney's fees and costs related to said losses or damages. Such indemnification and holding harmless shall include such losses or damages incurred by, or in connection with, acts or omissions of JoVE, its employees, agents or independent contractors.

13. **Fees.** To cover the cost incurred for publication, JoVE must receive payment before production and publication of the Materials. Payment is due in 21 days of invoice. Should the Materials not be published due to an editorial or production decision, these funds will be returned to the Author. Withdrawal by the Author of any submitted Materials after final peer review approval will result in a US\$1,200 fee to cover pre-production expenses incurred by JoVE. If payment is not received by the completion of filming, production and publication of the Materials will be suspended until payment is received.

14. **Transfer, Governing Law.** This Agreement may be assigned by JoVE and shall inure to the benefits of any of JoVE's successors and assignees. This Agreement shall be governed and construed by the internal laws of the Commonwealth of Massachusetts without giving effect to any conflict of law provision thereunder. This Agreement may be executed in counterparts, each of which shall be deemed an original, but all of which together shall be deemed to be one and the same agreement. A signed copy of this Agreement delivered by facsimile, e-mail or other means of electronic transmission shall be deemed to have the same legal effect as delivery of an original signed copy of this Agreement.

A signed copy of this document must be sent with all new submissions. Only one Agreement is required per submission.

CORRESPONDING AUTHOR

Name:

George S. Karagiannis, John S. Condeelis
Marek H. Oktay, David Entenbery

Department:

Anatomy & Structural Biology

Institution:

Albert Einstein College of Medicine

Title:

Dr Karagiannis is Post Doc (MD, PhD)

Signature:



Date:

12/28/2018

Please submit a **signed** and **dated** copy of this license by one of the following three methods:

1. Upload an electronic version on the JoVE submission site
2. Fax the document to +1.866.381.2236
3. Mail the document to JoVE / Attn: JoVE Editorial / 1 Alewife Center #200 / Cambridge, MA 02140

Dear Editor,

We have now corrected the editorial concerns:

1. Because of limitations on filming and video length, our filming limit for the protocol section is 2.75 pages. Please highlight 2.75 pages or less of the Protocol (including headers and spacing; see attached) that identifies the essential steps of the protocol for the video, i.e., the steps that should be visualized to tell the most cohesive story of the Protocol. Remember that non-highlighted Protocol steps will remain in the manuscript, and therefore will still be available to the reader.

Response: We have highlighted 2.75 pages or less of the protocol to be included in the video.

2. The protocol in section 1.2 (tumor transplantation) needs more information regarding animal welfare, as it involves survival surgery:

a) Please specify the use of vet ointment on eyes to prevent dryness while under anesthesia.

b) Discuss post-surgical treatment of animal, including recovery conditions and treatment for post-surgical pain.

c) Discuss maintenance of sterile conditions.

d) Please specify that the animal is not left unattended until it has regained sufficient consciousness to maintain sternal recumbency.

e) Please specify that the animal that has undergone surgery is not returned to the company of other animals until fully recovered.

Response: Comments are addressed in the following lines: (a) lines 165-166; (b) line 187; since this is a non-invasive surgery no pain-dealing medications are given. The antibiotics provided are outlined; (c) lines 170-171; (d-e) lines 183-185.

3. JoVE cannot publish manuscripts containing commercial language. This includes trademark symbols (™), registered symbols (®), and company names before an instrument or reagent. Please limit the use of commercial language from your manuscript and use generic terms instead. All commercial products should be sufficiently referenced in the Table of Materials and Reagents. For example: Matrigel, Corning, Henkel Adhesives, Becton Dickinson, Life Technologies, MouseOx, etc.

Response: all trademark symbols and company names before the reagents are now removed. The materials table is updated accordingly.

4. Please format citations as superscript numbers without brackets.

Response: Amended as requested.

5. Please ensure that the references appear as the following: [Lastname, F.I., LastName, F.I., LastName, F.I. Article Title. *Source*. Volume (Issue), FirstPage–LastPage (YEAR).] For more than 6 authors, list only the first author then et al. Also, please do not abbreviate journal titles.

Response: Amended as requested.